Functional genomics in *Dictyostelium*: MidA, a new conserved protein, is required for mitochondrial function and development

Patricia Torija, Juan J. Vicente, Tiago B. Rodrigues, Alicia Robles, Sebastián Cerdán, Leandro Sastre, Rosa M. Calvo and Ricardo Escalante*

Instituto de Investigaciones Biomédicas Alberto Sols. C.S.I.C./U.A.M., Calle Arturo Duperier 4, 28029 Madrid, Spain

*Author for correspondence (e-mail: rescalante@iib.uam.es)

Accepted 1 December 2005
Journal of Cell Science 119, 1154-1164 Published by The Company of Biologists 2006
doi:10.1242/jcs.02819

Summary

Genomic sequencing has revealed a large number of evolutionary conserved genes of unknown function. In the absence of characterized functional domains, the discovery of the role of these genes must rely on experimental approaches. We have selected 30 *Dictyostelium discoideum* genes of unknown function that showed high similarity to uncharacterized human genes and were absent in the complete proteomes from *Saccharomyces cerevisiae* and *S. pombe*. No putative functional motifs were found in their predicted encoded proteins. Eighteen genes were successfully knocked-out and three of them showed obvious phenotypes. A detailed analysis of one of them, *midA*, is presented in this report. Disruption of *midA* in *Dictyostelium* leads to pleiotropic defects. Cell size, growth rate, phagocytosis and macropinocytosis were affected in the mutant. During development, *midA*$^-$ cells showed an enhanced tendency to remain at the slug stage, and spore viability was compromised. The expression of MidA fused to GFP in *midA*$^-$ strain rescued the phenotype and the fused protein was located in the mitochondria. Although cellular oxygen consumption, mitochondrial content and mitochondrial membrane potential were similar to wild type, the amount of ATP was significantly reduced in the mutant suggesting a mitochondrial dysfunction. Metabolomic analysis by natural-abundance ^{13}C-nuclear magnetic resonance has shown the lack of glycogen accumulation during growth. During starvation, mutant cells accumulated higher levels of ammonia, which inhibited normal development. We hypothesize that the lack of MidA reduces mitochondrial ATP synthetic capacity and this has an impact in some but not all energy-dependent cellular processes. This work exemplifies the potential of *Dictyostelium* as a model system for functional genomic studies.

Key words: *Dictyostelium*, Functional genomics, Mitochondrial dysfunction, Genes of unknown function

Introduction

The sequence of complete genomes has revealed a large proportion of genes of unknown function conserved during evolution. Even for simple organisms with small genomes, such as prokaryotes, the proportion of genes of unknown function is higher than 35% (Doerks et al., 2004). Some of these uncharacterized proteins are highly conserved among distant organisms, suggesting that they play important roles. Comparative and functional genomics allow the study of conserved genes in simple organisms as the first step towards the characterization of these new genes. We have initiated a direct approach to the characterization of a subset of such genes using the social amoebae *Dictyostelium discoideum*, whose genome has been completely sequenced (Eichinger et al., 2005). The social amoebae are exceptional in their ability to form a multicellular organism by aggregation of solitary cells. The differentiation program is triggered by starvation and leads to the formation of a fruiting body composed of spores supported by a stalk (Escalante and Vicente, 2000). During growth, *Dictyostelium* amoeba feeds on bacteria and yeasts, ingesting them by phagocytosis and digesting them in lysosomes. Strains capable of growing in liquid medium in the absence of bacteria were selected for experimental convenience. In these strains, fluid-phase uptake is accomplished by macropinocytosis, which is similar but not identical to phagocytosis and involves the formation of large vacuoles termed macropinosomes (Cardelli, 2001). Once the developmental program is initiated, cells are starved during the whole process from aggregation to fruiting body formation. The glycogen accumulated during growth is used up in the differentiation process and the storage of other metabolites in the spores, such as glutamine and trehalose, is believed to be necessary to resist adverse environmental conditions.

Genome-wide collections of yeast mutants are undoubtedly helping in the characterization of new genes, some of them connected to human diseases (Mager and Winderickx, 2005). However, many genes that are present in higher organisms are absent in yeast. Several aspects of *Dictyostelium* biology, including phagocytosis, cell motility, chemotaxis, cell signaling, differentiation and morphogenesis, involve biological processes that are closer to higher organisms than to unicellular protists. At the molecular level, this similarity is translated into the presence of genes and signaling pathways conserved between *Dictyostelium* and higher eukaryotes but

not present in yeast (Williams et al., 2005). Some examples include the glycogen synthase kinase (GSKA), which controls cell differentiation in metazoan and *Dictyostelium* (Schilde et al., 2004), or the *Dictyostelium* β-catenin homologue that is, like in metazoans, involved in both in cytoskeleton and signaling (Coates et al., 2002; Grimson et al., 2000). The SH2 signaling pathway involving the transcriptional regulator STAT (signal transducers and activators of transcription) is also present in the social amoeba (Kawata et al., 1997), where it plays essential roles in multiple aspects of development. *Dictyostelium* is, therefore, an ideal system to address the function of uncharacterized conserved genes not present in the yeast models. In accordance to this rationale, we have selected genes showing high similarity between *Dictyostelium* and human, but were absent in yeasts (*S. cerevisise* and *S. pombe*). Further selection was performed by discarding those genes containing putative well-characterized functional domains using the Pfam database (http://pfam.wustl.edu/). Manual inspection of the remaining genes allowed a final selection of 66 conserved genes not previously characterized in any experimental model system. A systematic knockout approach is being performed and, so far, 18 genes have been successfully disrupted. Among them, three showed obvious phenotypes and were selected for detailed study. In this report we describe the characterization of one of them, *midA* (for mitochondrial dysfunction gene A), a conserved gene from α-proteobacteria to humans.

Results

Knockout analysis of genes of unknown function in *Dictyostelium*

Knockout vectors for 30 genes of unknown function were constructed and transfected in *Dictyostelium* as described in Materials and methods. These genes showed high similarity to uncharacterized human genes (E-values equal or lower than e-20) and no similar genes were found in *S. cerevisiae* and *S. pombe* with an E-value lower than e-2. Eighteen genes were successfully disrupted and three of them showed obvious phenotypes and were selected for further study. Analysis of one of them, *midA*, is presented in this report. The other two are being studied and will be described elsewhere. Homologous recombination was not successful for the remaining 12 genes after the analysis of at least 100 transfected clones for each one. Disruption of these genes might be deleterious for growth or, alternatively, their loci were located in regions of low frequency of recombination.

Table 1 shows *midA*, the *Dictyostelium* genes that were disrupted and did not show obvious phenotypes, together with their human homologues. The insertion of the blasticidine-resistance (BS)-cassette is located in the coding region of each gene as indicated. Although growth and development under standard experimental conditions were unaffected in these mutants (data not shown), this collection might serve as a resource for testing any specific phenotype in future studies. As shown in Table 1, the human homologues of two of these genes (*DDB0232147* and *DDB0232152*) have been cataloged into the human KIAA database (Kikuno et al., 2004), which comprises a group of large human new genes. Two other closely related *Dictyostelium* genes (*DDB0232151* and *DDB0232154*) show similarity to the Pfam domain DUF647, which corresponds to a conserved domain of unknown function. *DDB0232156* and *DDB0229859* show similarity to human genes involved in genetic diseases but the precise function of the encoded proteins remains poorly characterized. During the course of our project new data have been reported in relation with the mammalian homologues of *DDB0232149* and *DDB0232141*. *DDB0232149* shows similarity to the Pfam domain TH1 that is present in a group of highly conserved metazoan proteins and has been shown to function as a negative regulator of A-Raf kinase (Liu et al., 2004). However, the human homologue to *DDB0232141*, *UFC1*, is a new component of an ubiquitin-like (UBL) post-translational modifiers (Komatsu et al., 2004).

MidA codes for a conserved uncharacterized protein

Dictyostelium midA (*DDB0232140*) encodes a protein of

Table 1. *midA* and other disrupted genes in *Dictyostelium* with no obvious phenotype

DictyBase ID	Total aa/ site of insertion	Human protein	E-value	Characteristics
DDB0232140	425/77	NP_653337	1e-60	MidA
DDB0232141	164/135	CAH72141	8e-46	Ufc1
DDB0232143	366/207	CAI14128	2e-39	n.p.c.d.
DDB0232144	715/233	AAH40291	1e-82	n.p.c.d.
DDB0232146	794/291	CAI12688	1e-20	n.p.c.d.
DDB0232147	1133/794	BAA76798	5e-29	n.p.c.d. KIAA0954
DDB0232148	260/92	AAY15088	1e-42	n.p.c.d.
DDB0232149	660/249	CAB64339	2e-89	TH1 domain (Pfam 04858)
DDB0232150	930/375	BAB85063	2e-72	n.p.c.d.
DDB0232151	527/153	BAD96633	5e-57	DUF647 (Pfam 04884)
DDB0232152	2117/501	BAA20779	2e-22	n.p.c.d. KIAA0321
DDB0232153	1479/87	BAA25518	2e-28	n.p.c.d.
DDB0232154	567/183	BAD96633	3e-25	DUF647 (Pfam 04884)
DDB0232155	128/23	CAI22059	4e-21	n.p.c.d.
DDB0232156	688/327	NP_579877	2e-21	n.p.c.d. Wolf-Hirschhorn Syndrome (OMIM#194190)
DDB0229859	619/214	AAH04865	4e-101	n.p.c.d. Cleft lip and palate (OMIM#604783)

n.p.c.d.: no putative conserved domains.

unknown function that shows high similarity to the uncharacterized human protein PRO1853 (GenBank accession number NP_653337) located in chromosome 2. A search at the National Center for Biotechnology Information (NCBI) conserved-domain database generated two entries for *Dictyostelium* MidA, corresponding to an uncharacterized conserved protein family (DUF185 and COG1565). One member of the family from the bacteria *Brucella melitensis* (AI3312) has been electronically annotated as a possible transcriptional regulator [helix-turn-helix (HTH) motif] (DelVecchio et al., 2002) but, as far as we know, no experimental data supports this possibility. In conclusion, no available data, either experimental or based on sequence conservation, suggest a possible function for the protein. The human homologue of MidA, PRO1853, is located between the polymorphic markers D2S1788 and D2S2328 that have been linked to an autosomal dominant form of chronic mucocutaneous candidiasis associated with thyroid disease (Atkinson et al., 2001). Highly similar proteins to the *Dictyostelium* MidA can also be recognized in other organisms (Table 2). The plant and metazoan proteins show the highest similarity and, interestingly, homologues are also present in prokaryotes, mainly alpha-proteobacteria. However, no similar proteins are present in the complete proteomes of *S.cerevisiae* and *S.pombe*, even though several other fungi homologues are widely represented. Fig. 1A shows the alignment of *Dictyostelium discoideum* MidA with the human hypothetical protein PRO1853 and the homologue from *Magnetospirillum magnetotacticum* alpha-proteobacteria. Despite the enormous evolutionary distance between these species, the level of identity lies between 32% and 34%. Two different insertional mutants were generated (Fig1B, the coding region of MidA is represented by open boxes). Gene targeting was confirmed by PCR (Fig. 1C), by using flanking oligonucleotides whose location is indicated in Fig. 1B. The loss of mRNA expression as a result of homologous recombination was also determined by northern blotting (Fig. 1D). Both strains gave identical phenotypes and KO2 was used for further characterization (KO1 and KO2 are two mutant strains generated by disruption of the *midA*-coding region by homologous recombination). The pattern of *midA* mRNA expression was determined in northern blots as shown in Fig. 1D. A single transcript was detected that showed high level of expression at the vegetative stage and the first hours of development, but decreased thereafter to barely detectable levels during the last stages of development. It should be noticed that, the expression of the human homologue PRO1853 is supported by expressed sequence tags (ESTs); transcript variants generated by alternative splicing encoding

Table 2. Phylogenetic distribution of MidA homologs

Organism	E-value	Eukaryote	Bacteria	GenBank accession number
Arabidopsis	7e-82	Plants		NP_189511
Drosophila	2e-64	Metazoa		EAL29091
Xenopus	8e-64	Metazoa		AAH72911
Mus musculus	2e-61	Metazoa		NP_082887
Rattus novergicus	4e-61	Metazoa		XP_216627
Cryptococcus	4e-61	Fungi		EAL21636
Magnetospirillum	1e-60		alphaproteobacteria	ZP_00207869
Homo sapiens	1e-60	Metazoa		NP_653337
Azospirillum	5e-59		alphaproteobacteria	AAM53573
Gallus gallus	2e-58	Metazoa		XP_419525
Anopheles	2e-56	Metazoa		EAA10494
Bradyrhizobium	1e-51		alphaproteobacteria	NP_774085
Wolbachia	1e-51		alphaproteobacteria	NP_966476
Aspergillus	4e-50	Fungi		EAA58016
Rhodospirillum	5e-50		alphaproteobacteria	ZP_00267883
Caenorhabditis	5e-50	Metazoa		CAE65039
Debaryomyces	9e-50	Fungi		XP_459587
Rhodopseudomonas	3e-49		alphaproteobacteria	NP_949695
Caulobacter	8e-49		alphaproteobacteria	NP_419310
Leishmania	2e-48	Protist		CAB55618
Bartonella	4e-48		alphaproteobacteria	YP_032019
Mesorhizobium	1e-46		alphaproteobacteria	NP_103963
Brucella	3e-46		alphaproteobacteria	NP_539404
Rickettsi	8e-46		alphaproteobacteria	ZP_00339788
Agrobacterium	2e-45		alphaproteobacteria	NP_355171
Ehrlichia	2e-45		alphaproteobacteria	ZP_00210648
Candida albicans	6e-44	Fungi		EAK93208
Rhodobacter	3e-43		alphaproteobacteria	ZP_00005955
Gibberella	4e-43	Fungi		EAA73838
Ustilago	6e-43	Fungi		EAK85285
Yarrowia	4e-42	Fungi		XP_502764
Magnaporthe	3e-41	Fungi		EAA56443
Sinorhizobium	2e-38		alphaproteobacteria	NP_386450
Novosphingobium	7e-37		alphaproteobacteria	ZP_00305054
Neurospora	4e-31	Fungi		XP_322269
Silicibacter	7e-26		alphaproteobacteria	ZP_00338636
Nostoc	2e-24		cyanobacteria	ZP_00111102
Trichodesmium	2e-21		cyanobacteria	ZP_00325587
Anabaena	7e-20		cyanobacteria	ZP_00161961

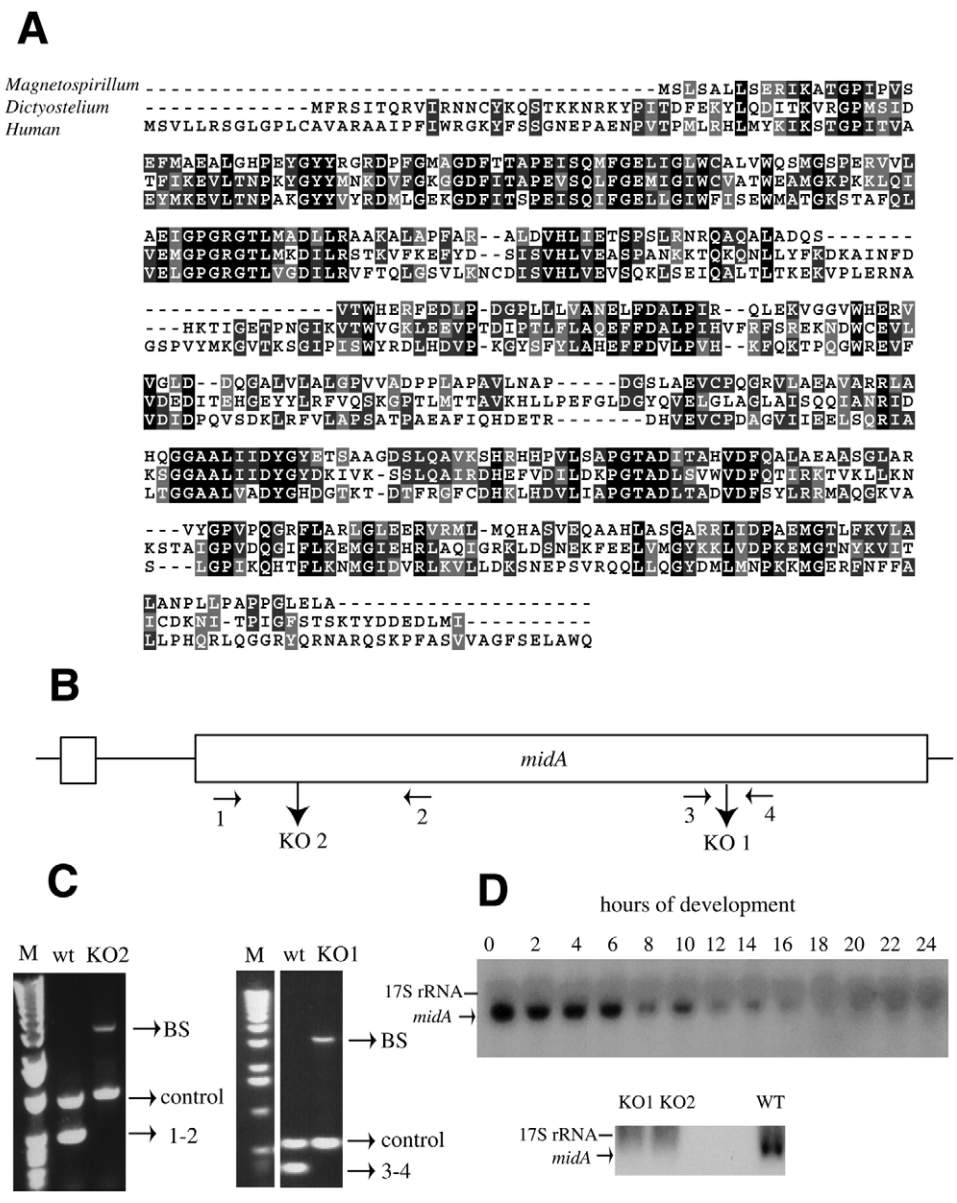

Fig. 1. MidA disruption and expression. (A) The sequence of *Dictyostelium* MidA protein was aligned with the human protein PRO1853 (GenBank accession number: NP_653337) and the most similar prokaryote protein from the alpha-proteobacteria *Magnetospirillum magnetotacticum* (GenBank accession number: ZP_00207869) using the ClustalW program. Black background corresponds to identical residues in three species, dark gray to identical residues in two species and light gray to similar residues. (B) The coding region of *midA* gene is depicted as two open boxes. The line between the open boxes represents an intron. KO1 and KO2 are two mutant strains generated by disruption of the *midA* coding region by homologous recombination at the indicated locations. Horizontal arrows show the oligonucleotides (1-4) used for checking the disruption of *midA* genomic locus in these strains. (C) Disruption of the *midA* gene was assessed by PCR. DNA from wild-type, KO1 (right panel) and KO2 (left panel) strains were subjected to PCR using the indicated oligonucleotides. A pair of oligonucleotides from an unrelated locus was used as internal control of the PCR reaction. The expected bands were absent in the KO strains due to the insertion of the BS-cassette. The upper bands in the KO samples (labeled as BS) corresponded to the inserted cassette. (D) RNA isolated at different times of development was hybridized with a radioactive probe derived from the coding sequence of the *midA* gene (upper panel). Lower panel shows the absence of *midA* mRNA in RNA samples from the KO strains isolated from vegetative stage.

different isoforms, have also been detected. These data are available at the Web resources from the NCBI (http://www.ncbi.nlm.nih.gov/UniGene/ESTProfileViewer.cgi?uglist=Hs.433466).

Disruption of MidA leads to pleiotropic defects in *Dictyostelium*

Loss of MidA leads to a wide repertoire of defects both at the vegetative stage and during development. Cell growth in association with bacteria was severely affected, as determined by the size of the clearing zone in SM plates (Fig. 2A). The same defect was observed in cells growing in shaking suspension with bacteria (data not shown). A moderate but reproducible reduction in cell growth rate was also seen in axenic culture where cell-doubling time increased from 10.5 hours in the parental strain to 14.7 hours in the mutant (Fig. 2B). The size of the cells, as determined by a direct measurement of their diameter, showed a significant average reduction of 20% (Fig. 2B). A large proportion of mutant cells had a diameter of 8-12 μm. However, wild-type cells displayed a wider distribution, with a significant proportion of cells with more than 12 μm (Fig. 2C). In accordance with this data, the amount of total protein per cell was also reduced to 70% from that of wild type. We wanted to determine whether the observed reduction in cell growth and size correlates with defects in nutrient uptake. In *Dictyostelium*, macropinocytosis accounts for most of fluid-phase uptake (Hacker et al., 1997) and phagocytosis is responsible for the uptake of particles such as bacteria (Raper, 1937). We found that both processes were affected by the absence of MidA (Fig. 2D). The uptake of fluorescent particles and fluorescent soluble material was reduced in the mutant after 30 minutes of incubation. Similar differences were found with 45 minutes of incubation with the fluorescent dyes (data not shown). Flow-cytometry also showed that the number of cells that were able to ingest multiple fluorescent microspheres was lower in *midA*$^{-}$ cells (Fig. 2E).

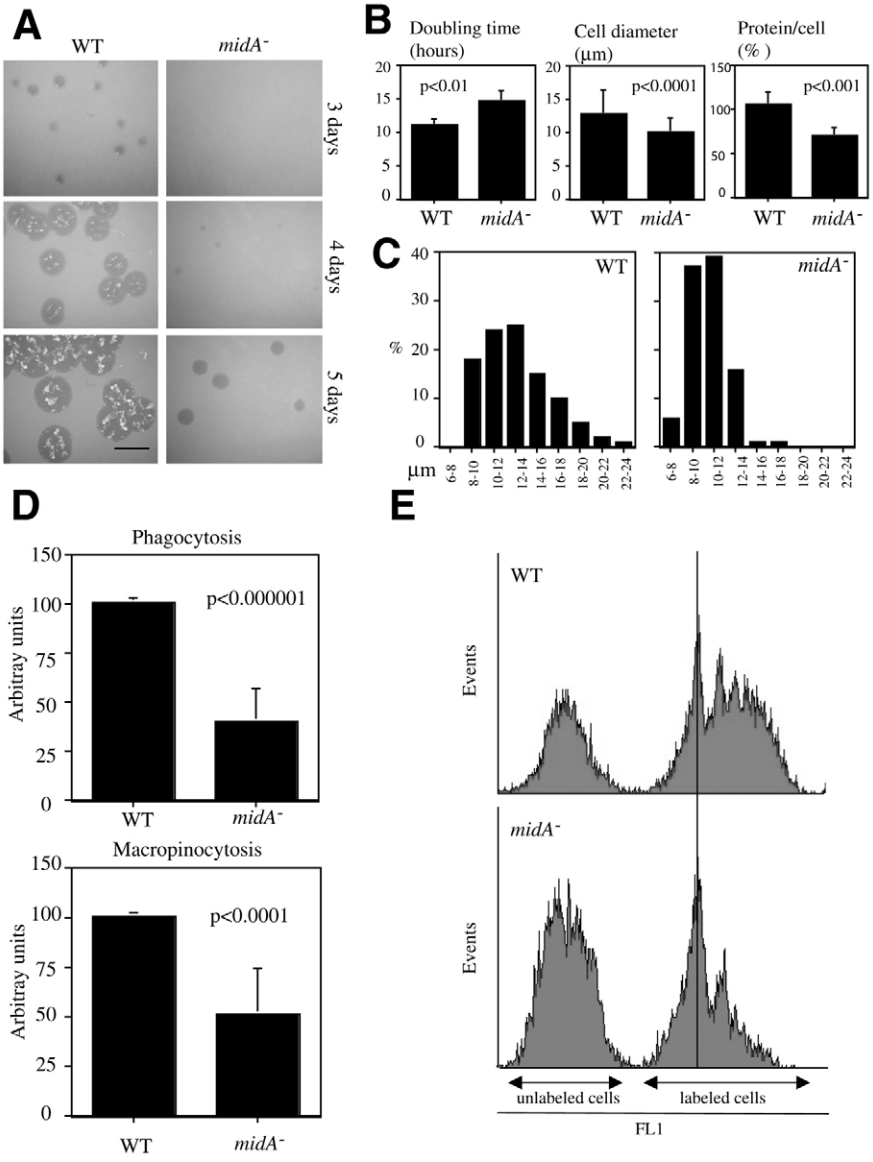

Fig. 2. Phenotype of *midA*⁻ at the vegetative stage. (A) Appropriate dilutions of wild-type and mutant *Dictyostelium* cells were plated in association with *Klebsiella aerogenes* in SM plates to determine differences in the size of the clearing zone. The plates were incubated at 22°C for the indicated times. Bar, 1 cm. (B) Growth rate in axenic medium, cell diameter and the amount of protein per cell were compared between the wild type and *midA*⁻ cells. Significance of differences is indicated by the *P* value shown inside the panels. (C) Proportion of cells (%) whose diameter is in the within the indicated sizes (μm). Most of the mutant cells had a diameter of 8-10 μm, whereas the majority of wild-type cells had a diameter of 10-14 μm. At least 200 cells were analyzed for each strain. (D) Axenically growing cells were exposed for 30 minutes to fluorescent beads (phagocytosis) or soluble fluorescent-dextran (macropinocytosis). The fluorimetry values were expressed as arbitrary units. The mean of three independent experiments is shown and the significance of differences indicated by the *P* value. (E) Representative flow-cytometry assay to determine the amount of fluorescent beads taken up by wild-type and *midA*⁻ cells. Both the total number of labeled cells and the proportion of cells with multiple beads were reduced in the mutant. For comparison, the vertical line is given as a reference.

Mutant and wild-type cells, previously grown in axenic media, were deposited on filters to study development. No differences were found in the timing of aggregation and tight mounds were formed at 10 hours after the onset of starvation (data not shown). Aggregation experiments, performed under submerged, low-density conditions, showed no differences between wild-type and *midA*⁻ cells. Long streams of aggregating polarized cells were formed under these conditions, suggesting no major defects in motility or chemotaxis in the mutant (data not shown).

The precise course of development in *Dictyostelium* depends on laboratory conditions such as light, pH and the strength of the buffer, which is used to neutralize weak bases generated by cell catabolism (Spudich, 1987). In non-buffered conditions with overhead light, a transient slug stage was induced in wild-type cells. After a short period of migration, slugs culminated at 26-48 hours (Fig. 3A). Mutants, however, became arrested and never culminated under these conditions. After several days, the structures seemed to flatten and became disorganized (Fig. 3A). We next used well-buffered conditions to induce direct culmination from the finger stage. Although the mutant structures were able to culminate under these conditions, they did so after a period of migration, that can be inferred by the sheath trails left behind by the slugs (see Fig. 3B). As expected, the filters in which wild-type cells developed did not show slime-sheath trails in the substratum, indicating the absence of a transient slug stage. In conclusion, our results suggest an increased tendency of the mutant strain to remain at the slug stage and, therefore, *midA*⁻ cell structures were only able to form fruiting bodies under strong culmination conditions. The spores contained in these structures were, nevertheless, defective as shown in Fig. 3C. Spores collected from 15-day-old fruiting bodies, a time necessary for complete maturation (Virdy et al., 1999), were rounder and less refringent under phase-contrast microscopy. To measure viability, these spores were treated with detergent and, after heating them to 42°C, plated in SM plates in association with bacteria. Almost 100% of wild-type spores were resistant to this treatment, whereas less than 10% of the mutant spores remained viable.

The loss of MidA leads to a mitochondrial dysfunction

Subcellular location of MidA was determined by the expression of green fluorescent protein (GFP) fused to the C-terminal end of the complete MidA *Dictyostelium* protein. The expression of this construct was driven by the actin15 promoter (represented in Fig. 4A). After transfection into *midA*⁻ cells, the resulting clones showed recovery in the growth rate in bacteria (Fig. 4B). Axenic growth, cell size and defects in development were also restored by the re-expression of the protein (data not shown), suggesting that the fusion protein is functional. GFP fluorescence was monitored in the recovered strains by confocal microscopy. GFP distribution showed a punctuate pattern that colocalized with the mitochondrial-specific marker MitoTracker Red (Fig. 4C). Transfection of the same construct in wild-type cells did not show any phenotype giving the same mitochondrial pattern. The merged images show the presence of few green areas with little or no red surrounding the MitoTracker Red staining (Fig. 4C, bottom panels). It has been previously reported that MitoTracker Red does not stain *Dictyostelium* mitochondria uniformly, being concentrated in spherical structures called sub-mitochondrial bodies (Van Es et al., 2001; Gilson et al., 2003). Moreover, a N-terminal mitochondrial signal was detected in MidA with the PSORT II program (Nakai and Horton, 1999). When this mitochondrial targeting signal was disturbed by fusion of GFP to the N-terminus of MidA, as previously described for other mitochondrial proteins (Meton et al., 2004), the fused product showed cytosolic staining and was not able to rescue the phenotype when expressed in *midA*⁻ mutant cells (data not shown). All together, our results strongly suggest that MidA is a mitochondrial protein, and targeting of the protein to this organelle is required for its function.

We next wanted to determine the possibility of a mitochondrial dysfunction that accounts for the observed complex phenotype in the mutant. The fluorescent marker MitoTracker Red (CMXRos) is incorporated into active mitochondria in a way that depends on the mitochondrial membrane potential (MMP) (Pendergrass et al., 2004). Staining with MitoTracker Green, by contrast, can be performed in fixed cells and is MMP-independent, being used to estimate mitochondrial cell content (Pendergrass et al., 2004). Cells were stained with these markers, observed by fluorescent microscopy and quantitative analysis was performed by fluorimetry. No considerable differences were found in the pattern or intensity of the staining when using any of these markers (Fig. 5A,B), suggesting that the amount of mitochondria per cell and the MMP was not affected in the mutant. Moreover, cellular oxygen consumption was also found to be unaffected in *midA*⁻ cells (Fig. 5D). However, the amount of ATP per cell was reduced to 70 % of that found in wild type, suggesting a mitochondrial defect in the efficiency of ATP production (Fig. 5C).

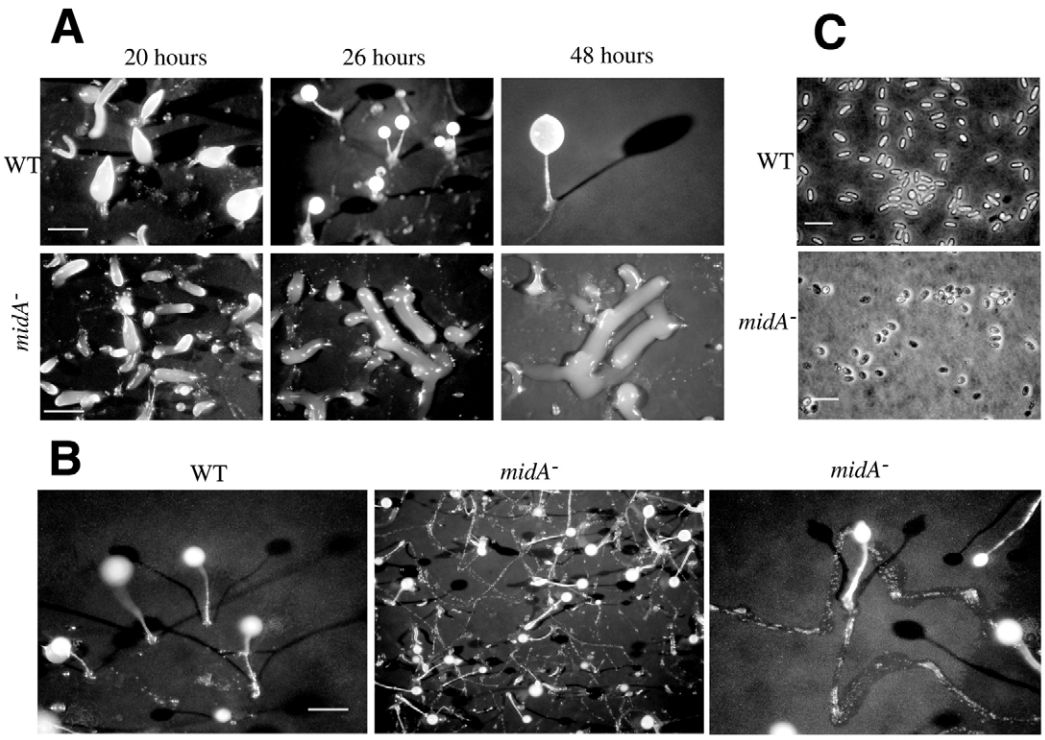

Fig. 3. Phenotype of *midA*⁻ during development. (A) Wild-type and mutant cells were deposited in nitrocellulose filter for development under overhead light at 22°C. The underlying cellulose pad was soaked with water and representative photographs are shown at the indicated times. Under these conditions (without buffer) the mutant cells were unable to form fruiting bodies. Bars, 0.5 mm. (B) Cells were deposited on filters as described before, but in this case the underlying pad was soaked with PDF buffer to induce direct culmination. Under these conditions *midA*⁻ is able to culminate after a period of migration. Notice the presence of slime-sheath trails left behind at the base of the fruiting bodies. Bars, 0.5 mm. (C) Spores taken from 15-day-old fruiting bodies and photographed with a phase-contrast microscope. Mutant cells are rounder and less refringent than wild-type cells. Bar, 10 μm.

The level of certain metabolites is affected in *midA* mutants

We next determined whether the mitochondrial dysfunction observed as a result of MidA disruption had major effects in the level of metabolites as determined by natural-abundance proton-decoupled ^{13}C-nuclear magnetic resonance (NMR) spectroscopy. The comparison of the spectra of $HClO_4$ extracts from cells grown to late exponential phase, depicted important differences in two metabolites (Fig. 6A). Glycogen, an endogenous store of carbohydrates, was completely absent in the mutant cells. However, glutamate, whose levels in wild-type cells were undetectable, showed a clear accumulation in *midA*$^-$ cells.

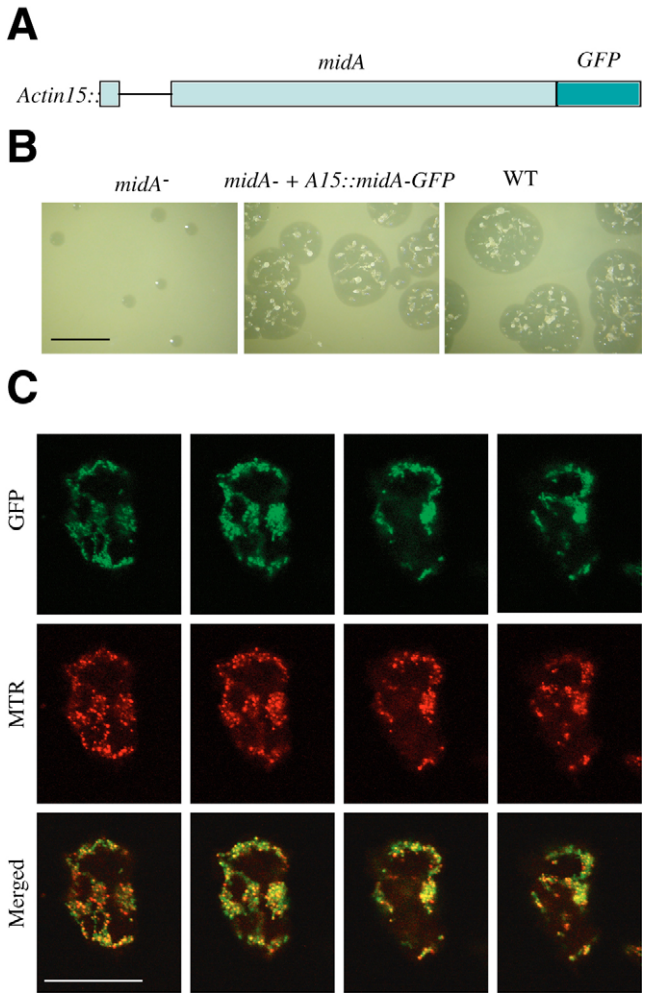

Fig. 4. MidA is a mitochondrial protein. (A) Scheme of the construct that was used for the expression of MidA fused to GFP. Coding sequences are depicted as open boxes and the intron by a thin line. The expression of the fused genes was driven by the actin 15 promoter. (B) Colony size after transfection of the construct *A15::midA-GFP* into *midA*$^-$ cells. The indicated strains were mixed with *Klebsiella aerogenes* and plated on SM plates. Photographs were taken after 5 days at 22°C. Bar, 1 cm. (C) Cells expressing midA fused to GFP were incubated with the mitochondrial marker MitoTracker Red, fixed and observed in a confocal microscope. Series of 2-μm confocal images from the same cell show GPF location in green and the mitochondrial marker in red. Colocalization can be seen in the merged images. Bar, 10 μm.

Ammonia is generated as a result of protein catabolism during starvation, and functions in *Dictyostelium* as a signaling molecule by repressing culmination (Schindler and Sussman, 1977). The level of ammonia is reduced at this stage of development, in part, by the induction of a glutamine synthetase that uses ATP to incorporate ammonia into glutamic acid generating glutamine, which is accumulated during development (Klein et al., 1990). The difficulties of the mutant structures to progress through culmination and also the reduced ATP levels led us to consider the possibility of abnormal accumulation of ammonia. We measured the amount of ammonia released into the cellulose pads underneath the filters during starvation and found that *midA*$^-$ cells accumulated a higher concentration of ammonia (Fig. 6B). Experimental reduction of ammonia levels, by using two absorbent pads underneath the filter instead of one, was able to rescue the delay in culmination (Fig. 6C). This is in agreement with the hypothesis that high levels of ammonia were responsible of the increased tendency of the *midA*$^-$ cell structures to remain at the slug stage.

Discussion

The social amoeba shares several biological aspects with animal cells, including cell motility, phagocytosis, cell differentiation and multicellular development. *Dictyostelium* is probably the simplest experimental model where these processes can be studied. We wanted to exploit this usefulness

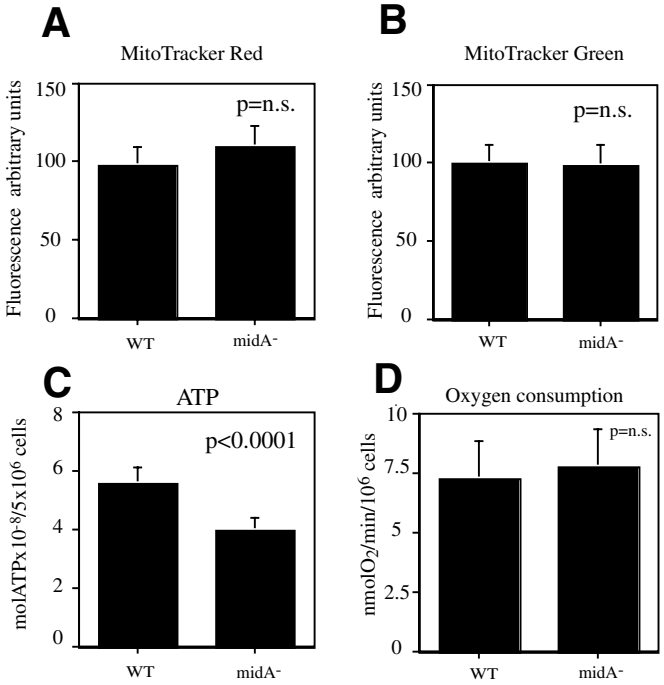

Fig. 5. Mitochondrial dysfunction in *midA*$^{-/-}$ cells. Mitochondria were stained with Mito Tracker Red (A) or Mito Tracker Green (B) and fluorimetric quantification of the respective fluorescence from similar numbers of wild type and mutant cells was carried out. (C) The amount of ATP was measured in a bioluminescence assay. (D) Cellular oxygen consumption from wild-type and *midA*$^-$ cells was measured in a Clark-type electrode. Significance of differences is indicated by the *P* value shown inside the panels; n.s., non-significant differences.

and tried to address the function of new conserved genes in *Dictyostelium*, focusing on those that were absent in other model organisms, such as yeast, that do not show these processes. Proteome comparison between human, *Dictyostelium*, *S. cerevisiae* and *S. pombe* revealed around 360 genes that are conserved in *Dictyostelium* and higher organisms but are absent in yeasts. Some of these might correspond to genes gained in the course of evolution to accomplish new functions, related with the aspects that *Dictyostelium* shares with higher organisms (as stated above). Others might have been lost in the yeast lineage. Gene-gain and -loss have shaped the genome of eukaryotes during evolution. Of those genes, 66 were found to contain no conserved functional domains that would allow homologue-based annotation. The detailed study of one of them, MidA, has allowed us to shed some light on the function of this conserved protein.

The level of similarity of *Dictyostelium* MidA with the alpha-proteobacterial homologues is comparable with or even higher than that observed for other eukaryotes. Since alpha-proteobacteria are believed to be the ancestors of mitochondria, these data suggest that *midA* genes have been present in the mitochondrial ancestor and were transferred to the nuclear genome. The mitochondrial genome encodes only a small fraction of the mitochondrial proteins, the remaining being encoded in the nuclear DNA. It is known from studies in yeast that, about half of the mitochondrial nuclear-encoded proteins have bacterial homologues, suggesting a massive transfer from the genome of the putative endosymbiont. The other half seems to be recruited from the nuclear genome because no homologues can be traced to bacteria (Andersson et al., 2003; Karlberg et al., 2000). Interestingly, most of the proteins with clear homologues in alpha-proteobacteria are involved in crucial functions, such as energy metabolism, or encode ribosomal proteins (Andersson et al., 2003). No MidA homologues seem to be present in the yeasts *S. cerevisiae* or *S. pombe*. However, similar proteins can be found in *Candida albicans* and other fungi, suggesting a specific gene lost in those species.

In this report we present the first functional data for the conserved protein MidA. We have shown that *Dictyostelium* MidA is a mitochondrial protein involved in bioenergetics. The lower levels of ATP found in the mutant argue in favor of a mitochondrial dysfunction. Since no differences were found between wild-type and mutant cells in the mitochondrial content, MMP and oxygen consumption, a decrease in the mitochondrial ATP synthetic capacity seems to be responsible for the phenotype. As a result of this specific mitochondrial

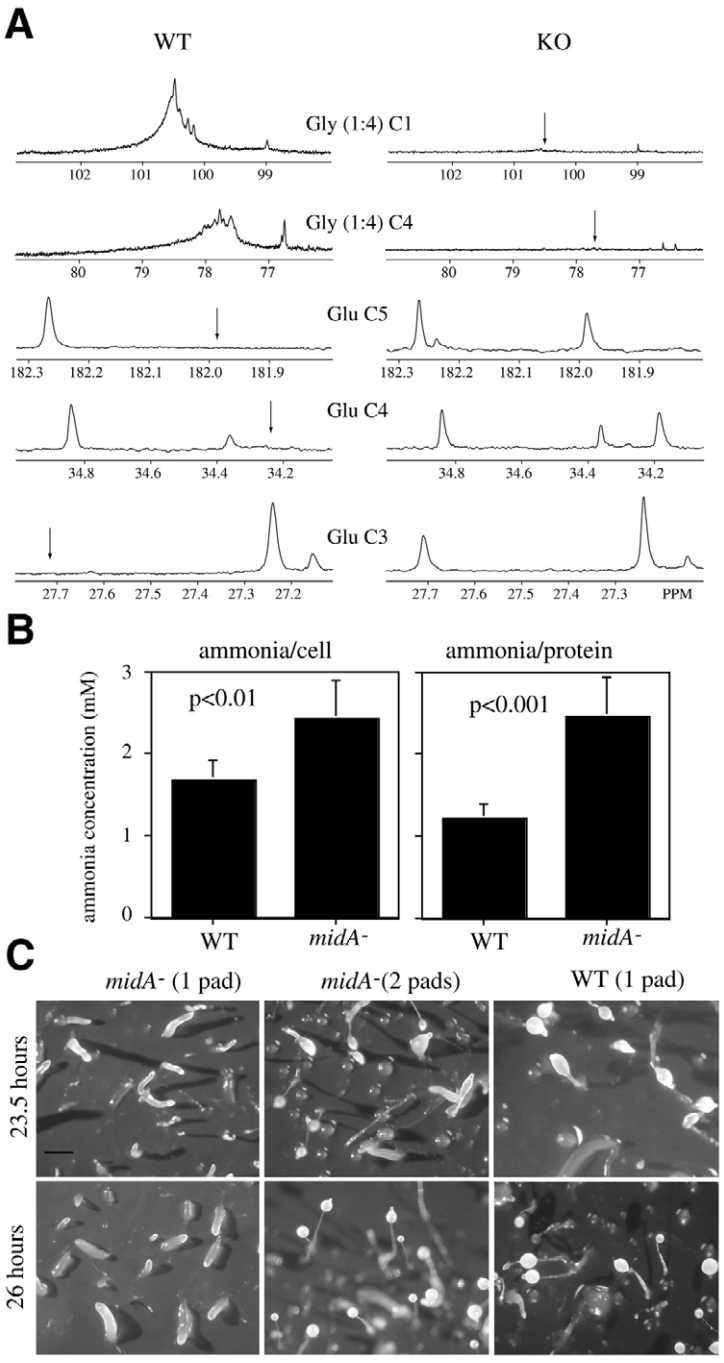

Fig. 6. Changes in the accumulation of glycogen, glutamate and ammonia. (A) Natural-abundance proton-decoupled ^{13}C-NMR spectra (125.13 MHz, 25°C, pH 7.2) of perchloric acid extracts from wild-type (WT) and mutant (KO) cells grown to late exponential phase. Resonances from carbons C1 (100.6 ppm) and C4 (77.8 ppm) of glycogen (Gly 1:4) and carbons C3 (27.7 ppm), C4 (34.2 ppm) and C5 (181.9 ppm) of glutamate (Glu) are shown in representative spectra of wild-type (left) and mutant cells (right). Arrows highlight the disappearance of glycogen and glutamate resonances. (B) Similar amount of wild-type and mutant cells were washed and deposited on nitrocellulose filters over cellulose pads. After 5 hours of starvation at 22°C, cells were taken off the filter for protein quantification, and the ammonia released to the underneath cellulose pad was determined by a colorimetric assay; ammonia concentration (mM) normalized to the number of cells (left panel) and total protein content (right panel). (C) Wild-type and mutant cells were deposited on filters for development with one or two PDF-soaked cellulose pads. Photographs were taken at the indicated times. When one cellulose pad was used under the filter, the wild-type cells culminated normally, whereas the mutant remained at the slug stage. This delay in culmination was rescued in *midA*$^{-}$ when two cellulose pads were used underneath the filter to dilute the secreted ammonia. Bar, 0.5 mm.

dysfunction, a wide repertoire of cellular functions is compromised in *Dictyostelium*: cell size, protein content, growth rate, phagocytosis, macropinocytosis and metabolism, as reflected on the levels of glycogen and glutamate. These defects might be adaptive responses of the cell to a low-energy status. Mammalian cells respond to impaired cellular energetics, such as restricted nutrient supply or conditions of increased energy demand, in different ways. The best-known mechanism involves the AMP-activated protein kinase (AMPK) that controls the metabolic status of the cell by activating the catabolic pathways and downregulating ATP-depending anabolic pathways (Hardie and Carling, 1997; Young et al., 2005). In mammalian cells, AMPK phosphorylates the glycogen synthase, thereby inhibiting its activity, which leads to a depletion of the storage of glucose in the form of glycogen (Jorgensen et al., 2004). In *Dictyostelium*, glycogen is accumulated during growth and its levels decrease during differentiation (Hames et al., 1972). Glycogen is believed to serve as fuel and to provide precursors for structural components, such as cellulose, during terminal differentiation (Harris and Rutherford, 1976; Rutherford and Harris, 1976). Its absence in *midA*$^{-}$ cells might therefore compromise diverse cellular functions in subsequent stages. The reduced cell size and protein content of the mutant and its reduced growth rate might also be the consequence of the limited biosynthetic capacity of the cells. Interestingly a petite phenotype in yeast is commonly associated with defects in mitochondrial DNA replication, transcription, translation or protein assembly (Contamine and Picard, 2000).

Phagocytosis and macropinocytosis result in the internalization of particles and fluids and are required in diverse functions, from nutrition in simple eukaryotes, such as *Dictyostelium*, to immunity in mammals performed by neutrophils and macrophages. Our results show that these processes are impaired in *midA*$^{-}$ cells, suggesting a requirement for functional mitochondria. This is not the first example relating mitochondrial function to phagocytosis. Reduced phagocytic activity has been reported in macrophages as a consequence of mitochondrial dysfunction induced by ketamine, an intravenous anesthetic (Chang et al., 2005). In contrast to macrophages, the disruption of mitochondrial function in neutrophils has no effect on phagocytosis (Fossati et al., 2003). A plausible explanation is that neutrophils seem to rely on glycolysis for energy production. Therefore, their requirement for active mitochondria is lower, allowing them phagocytose efficiently under anaerobic conditions (Fossati et al., 2003). It might be argued that phagocytosis and macropynocytosis are impaired as a direct consequence of the low availability of cellular energy in the form of ATP, necessary for cytoskeleton rearrangements during phagosome and macropynosome formation. However, other probably more energy-demanding processes that also involve the cytoskeleton, such as cell motility and chemotaxis, do not seem to be compromised in the mutant. Interestingly, macrophage migration was not affected by mitochondrial dysfunction induced by ketamine (Chang et al., 2005). The partial impairment of phagocytosis might be explained by the overall reduction in biosynthetic metabolic activity of the cell that would downregulate the uptake of nutrients.

Previous studies in *Dictyostelium* have shown the involvement of mitochondria in cell differentiation and pattern formation (Chida et al., 2004; Kotsifas et al., 2002; Matsuyama and Maeda, 1998; Wilczynska et al., 1997). Cells with reduced amount of mitochondrial DNA were obtained by exposing *Dictyostelium* cells to ethidium bromide (Chida et al., 2004). When starved, these cells showed a delay in development and, more remarkably, the structures became arrested at the slug stage, a phenotype that resembles the one observed in *midA*$^{-/-}$ cells.

Dictyostelium development takes place in the absence of exogenous nutrients and this results in the generation of ammonia from protein catabolism (Gregg et al., 1954). Ammonia needs to be kept at low concentrations during development because it functions as an inhibitor of the transition from slug migration to fruiting body formation (Schindler and Sussman, 1977). Ammonia detoxification in *Dictyostelium* is accomplished by diffusion to the media and by a metabolic pathway that converts α-ketoglutarate to glutamate with the incorporation of one ammonia molecule. Another molecule of ammonia is then incorporated to glutamate by the action of a glutamine synthetase to yield glutamine. According to this, the amount of ammonia has been previously shown to decrease during culmination (Wilson and Rutherford, 1978), whereas the activity of glutamine synthetase increases at this time of development (Dunbar and Wheldrake, 1997). Only the last step of conversion of glutamate to glutamine consumes ATP. Glutamate on the other hand is used in biosynthetic metabolic pathways of amino acids and purines. In a cellular scenario in which the biosynthetic pathways are inhibited (as suggested by the absence of glycogen) and the availability of ATP is limited, glutamate is expected to be accumulated – as observed by us in the mutant. Moreover, the increased accumulation of ammonia in *midA*$^{-}$ cells during starvation might be the result of the contribution of an increased catabolic metabolism and partially impaired detoxification pathways, such as the conversion of glutamate to glutamine. Our experiments suggest that those increased levels of ammonia might be responsible for the defects in culmination. However, we can not rule out the possibility of an additional component of ammonia hypersensitivity in the mutant, as described for other slugger mutants (Gee et al., 1994). We have also shown a sporulation defect in the mutant. It is intriguing that the expression pattern of *midA* shows no detectable levels of mRNA during late differentiation. It is plausible that previous accumulation of certain metabolites, such as glycogen and glutamine, during growth and early development are later necessary for terminal differentiation. According to this, it was described that glutamine and trehalose are accumulated to large amounts during development to reach the highest levels in the spores (Klein et al., 1990). Further investigation will be required to fully understand the role of MidA in sporulation.

In conclusion, we hypothesize that the lack of MidA reduces mitochondrial ATP synthetic capacity and also that this has an impact in some, but not all, energy-depending cellular processes. Its involvement in bioenergetics, a crucial mitochondrial function, and the presence of highly homologous proteins in alpha-proteobacteria are consistent with the possibility of an endosymbiontic origin, as described for other mitochondrial proteins encoded in the nuclear genome.

Materials and Methods

Dictyostelium cell culture, transfection and development

Cells were grown axenically in HL5 medium (14 g/l tryptone, 7 g/l yeast extract, 0.35 g/l Na_2HPO_4, 1.2 g/l KH_2PO_4, 14 g/l glucose, pH 6.5) or in association with *Klebsiella aerogenes* in SM plates (10 g/l glucose, 1 g/l yeast extract, 10 g/l peptone, 1 g/l $MgSO_4{\cdot}6H_20$, 1.9 g/l KH_2PO_4, 0.6 g/l K_2HPO_4, 20 g/l agar, pH 6.5) (Sussman, 1987). Transfections were carried out by electroporation as described previously (Pang et al., 1999). For synchronous development, axenically growing cells were separated from culture media by centrifugation, resuspended in water or PDF buffer and deposited on nitrocellulose filters (Shaulsky and Loomis, 1993). Spore viability after detergent and heat treatments was evaluated as described previously (Nuckolls et al., 1996; Shaulsky and Loomis, 1993).

Generation of mutant strains

DNA fragments ranging from 2-2.5 kb containing the genes to be disrupted were amplified by PCR from genomic DNA and cloned in pGEMt easy vector (PROMEGA) according to the manufacturer's instructions. Insertion of the blasticidin-resistance (BS)-cassette was performed by in vitro transposition using the vector and the procedure described previously (Abe et al., 2003). The constructs containing the flanking regions and the transposon were amplified by PCR and the products were transformed in *Dictyostelium* cells by electroporation. Transfected cells were plated in association with bacteria for clonal isolation and screened for homologous recombination by PCR, with oligonucleotides surrounding the site of insertion. The DNA of the transfected clones used for PCR was isolated from cells of the growing zone from SM plates using the Master amp DNA extraction solution from Epicentre.

GFP expression constructs and confocal studies

The *midA* gene was amplified from genomic DNA using oligonucleotides that contain sites for the restriction enzyme *Bam*HI. The fragment was cloned in pGEMt-easy vector and sequenced to check for possible polymerase errors. The fragment was subsequently cloned into the *Bam*HI site of the green fluorescent protein (GFP) vector pDEX-GFP kindly provided by Francisco Rivero (University of Cologne, Germany). The construct (MidA-GFP), driven by an actin15 promoter, contained the complete MidA coding region fused to GFP. After isolation of transfected clones, cells were stained with Mitotracker Red, fixed and imaged with a laser scanning TCS-NT Leica confocal microscope.

Phagocytosis and macropynocytosis assays

Cells growing in axenic media were adjusted to 10^6 cells/ml and incubated with 1 μl of fluorescent latex beads/ml (Fluoresbrite™ from Polysciences) or 0.5 mg/ml of FICT-dextran for 30 or 45 minutes in shaking culture. After incubation, cells were collected and washed three times by centrifugation at 150 ***g*** for 4 minutes with cold HL5. After the final centrifugation, cells were lysed in buffer containing 0.3% Triton X-100 and the fluorescence of each sample was measured in a luminescence spectrometer LS50 (Perkin Elmer). Fluorimetry parameters of excitation and emission were set to 441/486 for the fluorescent beads and to 485/515 for the FICT-dextran.

Flow-cytometry was used to determine the phagocytosis rate in wild-type and knockout strains. Cells growing at a density of $1\text{-}3\times10^6$ cells/ml were incubated with 1 μl of fluorescent latex beads (Fluoresbrite) in 1 ml of fresh HL5 during 1 hour in shaking culture at 150 ***g***. After centrifugation (5 minutes) and washing, cells were resuspended in phosphate buffer and fluorescence activated cell sorting (FACS; Becton Dickinson) analyses was carried out. For each sample, 10,000 cells were counted; fluorescence data were analyzed with WinMDI software.

Staining with mitochondrial-specific probes

Cells growing in axenic media were stained with MitoTraker Red (Molecular Probes) in HL5 at a final concentration of 100 nM during 30 minutes in shaking culture. Cells were centrifuged, washed with HL5, and deposited on a microscope coverslide. After 10 minutes, to allow the attachment of cells to the slide, they were fixed for 15 minutes with 3.7% formaldehyde in HL5. After fixation, cells were washed twice with PBS (133 mM sodium chloride; 10 mM sodium potassium phosphate, pH 7.4) and mounted with 80% glycerol for observation. Staining with MitoTracker Green (Molecular Probes) was performed over cells previously fixed with formaldehyde. MitoTracker Green was used at a final concentration of 40 nM in PBS during 10 minutes, washed and mounted for microscopy. For quantification of fluorescence, 10^6 cells were stained in suspension with the mitochondrial specific probes at the same concentration as described before. Staining with MitoTracker Red was performed on living cells and the staining with MitoTracker Green on fixed cells. The pertinent washes were performed by gentle centrifugation (5 minutes at 150 ***g***) and subsequent resuspension of the cells. Fluorescence was measured in a fluoreskan ascent (Lab Systems).

Measurements of ATP- and oxygen-consumption and ammonia

Dictyostelium cells growing in axenic media were washed and resuspended in water. TCA was added to a final concentration of 1% (v/v) and cells were incubated for 10 minutes at room temperature while vortexing several times. After centrifugation (5 minutes at 150 ***g***), ATP levels were measured in the supernatant with the ATP Bioluminescence Assay Kit CLSII from Roche. Oxygen consumption was measured polarographically using a Clark-type oxygen electrode. Cells were washed, resuspended in PDF buffer and placed in the respiration chamber at room temperature. Oxygen consumption was measured for the duration of 5 minutes after equilibration of the electrode. Ammonia levels were determined using a colorimetric test from MERK (Aquamerk Ammonium Test). Cellulose pads were incubated in 50 ml of water for 30 minutes to allow diffusion of ammonia. Concentration of ammonia in the solution was then determined according to manufacturer's instructions, except for quantification of the colorimetric reaction that was performed in an ELISA spectrophotometer at 595 nm by extrapolation to standards of known ammonia concentration.

NMR spectroscopy

Perchloric acid extracts from cells grown to late exponential phase were obtained as described previously, neutralized with KOH, lyophilized, and resuspended in ^2H_2O (99.9% ^2H) prior to high-resolution ^{13}C-nuclear magnetic resonance (NMR) analysis (Klein et al., 1990). Natural-abundance proton-decoupled ^{13}C-NMR spectra from these extracts were obtained at 11.9 Tesla (125.13 MHz, 25°C, pH 7.2) with a Bruker AVANCE 500 wide bore NMR spectrometer using a commercial (5 mm) triple resonance probe (^1H, ^{13}C, ^2H) optimized for direct ^{13}C-NMR detection. Acquisition conditions were: π/3 pulses; 30.0 kHz spectral width; 1.09 seconds acquisition time; 64k words data table; and 6.0 seconds recycling time. ^{13}C-spectra were the sum of 40,000 free induction decays. Proton decoupling was gated on only during the acquisition using a broadband composite pulse decoupling sequence. Resonance assignments were based on literature values and on the addition of internal standards (Cerdán et al., 1990; Klein et al., 1990). Chemical shifts were calibrated with an external reference of dioxane [10% vol/vol, 67.4 parts per million (ppm)]. ^{13}C-spectra were analyzed using the program NUTS (Acorn, Freemont, CA, USA), as implemented in an Intel Centrino Platform.

Statistical analysis

Results are shown as mean values with standard deviation (s.d.) from duplicates or triplicates of at least three independent experiments. Significance of differences between groups were determined by Student's *t*-test.

We thank Carlos Quijano from our bioinformatics facility for his help in the proteome analysis. T.B.R. was supported by a fellowship from Fundação para a Ciência e Tecnologia/Ministério da Ciência e Ensino Superior-Portugal. This work was supported by grant BMC2003-02814 from the Spanish Ministerio de Educación y Ciencia. Sequence data for *Dictyostelium* were obtained from the Genome Sequencing Centers of the University of Cologne, Germany, the Institute of Molecular Biotechnology, Department of Genome Analysis, Jena, Germany, the Baylor Collage of Medicine in Houston, Texas, and the Sanger Center in Hinxton, Cambridge, UK.

References

Abe, T., Langenick, J. and Williams, J. G. (2003). Rapid generation of gene disruption constructs by *in vitro* transposition and identification of a *Dictyostelium* protein kinase that regulates its rate of growth and development. *Nucleic Acids Res.* **31**, E107.

Andersson, S. G., Karlberg, O., Canback, B. and Kurland, C. G. (2003). On the origin of mitochondria: a genomics perspective. *Philos. Trans. R. Soc. Lond. B Biol. Sci.* **358**, 165-177.

Atkinson, T. P., Schaffer, A. A., Grimbacher, B., Schroeder, H. W., Jr, Woellner, C., Zerbe, C. S. and Puck, J. M. (2001). An immune defect causing dominant chronic mucocutaneous candidiasis and thyroid disease maps to chromosome 2p in a single family. *Am. J. Hum. Genet.* **69**, 791-803.

Cardelli, J. (2001). Phagocytosis and macropinocytosis in *Dictyostelium*: phosphoinositide-based processes, biochemically distinct. *Traffic* **2**, 311-320.

Cerdán, S., Kunnecke, B. and Seelig, J. (1990). Cerebral metabolism of [1,2-$^{13}C_2$] acetate as detected by in vivo and in vitro ^{13}C NMR. *J. Biol. Chem.* **265**, 12916-12926.

Chang, Y., Chen, T. L., Sheu, J. R. and Chen, R. M. (2005). Suppressive effects of ketamine on macrophage functions. *Toxicol. Appl. Pharmacol.* **204**, 27-35.

Chida, J., Yamaguchi, H., Amagai, A. and Maeda, Y. (2004). The necessity of mitochondrial genome DNA for normal development of *Dictyostelium* cells. *J. Cell Sci.* **117**, 3141-3152.

Coates, J. C., Grimson, M. J., Williams, R. S., Bergman, W., Blanton, R. L. and Harwood, A. J. (2002). Loss of the beta-catenin homologue aardvark causes ectopic stalk formation in *Dictyostelium*. *Mech. Dev.* **116**, 117-127.

Contamine, V. and Picard, M. (2000). Maintenance and integrity of the mitochondrial genome: a plethora of nuclear genes in the budding yeast. *Microbiol. Mol. Biol. Rev.* **64**, 281-315.

DelVecchio, V. G., Kapatral, V., Redkar, R. J., Patra, G., Mujer, C., Los, T., Ivanova,

N., Anderson, I., Bhattacharyya, A., Lykidis, A. et al. (2002). The genome sequence of the facultative intracellular pathogen *Brucella melitensis*. *Proc. Natl. Acad. Sci. USA* **99**, 443-448.
Doerks, T., von Mering, C. and Bork, P. (2004). Functional clues for hypothetical proteins based on genomic context analysis in prokaryotes. *Nucleic Acids Res.* **32**, 6321-6326.
Dunbar, A. J. and Wheldrake, J. F. (1997). Effect of the glutamine synthetase inhibitor, methionine sulfoximine, on the growth and differentiation of *Dictyostelium discoideum*. *FEMS Microbiol. Lett.* **151**, 163-168.
Eichinger, L., Pachebat, J. A., Glockner, G., Rajandream, M. A., Sucgang, R., Berriman, M., Song, J., Olsen, R., Szafranski, K., Xu, Q. et al. (2005). The genome of the social amoeba *Dictyostelium discoideum*. *Nature* **435**, 43-57.
Escalante, R. and Vicente, J. J. (2000). *Dictyostelium discoideum*: a model system for differentiation and patterning. *Int. J. Dev. Biol.* **44**, 819-835.
Fossati, G., Moulding, D. A., Spiller, D. G., Moots, R. J., White, M. R. and Edwards, S. W. (2003). The mitochondrial network of human neutrophils: role in chemotaxis, phagocytosis, respiratory burst activation, and commitment to apoptosis. *J. Immunol.* **170**, 1964-1972.
Gee, K., Russell, F. and Gross, J. D. (1994). Ammonia hypersensitivity of slugger mutants of *D. discoideum*. *J. Cell Sci.* **107**, 701-708.
Gilson, P. R., Yu, X., Hereld, D., Barth, C., Savage, A., Kiefel, B. R., Lay, S., Fisher, P. R., Margolin, W. and Beech, P. L. (2003). Two Dicyostelium orthologs of the prokaryotic cell division protein FtsZ localize to mitochondria and are required for the maintenance of normal mitochondrial morphology. *Eukaryot. Cell* **2**, 1315-1326.
Gregg, J. H., Hackney, A. L. and Krivanek, J. O. (1954). Nitrogen metabolism of the slime mold *Dictyostelium discoideum* during growth and morphogenesis. *Biol. Bull.* **107**, 226-235.
Grimson, M. J., Coates, J. C., Reynolds, J. P., Shipman, M., Blanton, R. L. and Harwood, A. J. (2000). Adherens junctions and beta-catenin-mediated cell signalling in a non-metazoan organism. *Nature* **408**, 727-731.
Hacker, U., Albrecht, R. and Maniak, M. (1997). Fluid-phase uptake by macropinocytosis in *Dictyostelium*. *J. Cell Sci.* **110**, 105-112.
Hames, B. D., Weeks, G. and Ashworth, J. M. (1972). Glycogen synthetase and the control of glycogen synthesis in the cellular slime mould *Dictyostelium discoideum* during cell differentiation. *Biochem. J.* **126**, 627-633.
Hardie, D. G. and Carling, D. (1997). The AMP-activated protein kinase–fuel gauge of the mammalian cell? *Eur. J. Biochem.* **246**, 259-273.
Harris, J. F. and Rutherford, C. L. (1976). Localization of glycogen synthetase during differentiation of presumptive cell types in Dictyostelium discoideum. *J. Bacteriol.* **127**, 84-90.
Jorgensen, S. B., Nielsen, J. N., Birk, J. B., Olsen, G. S., Viollet, B., Andreelli, F., Schjerling, P., Vaulont, S., Hardie, D. G., Hansen, B. F. et al. (2004). The alpha2-5′AMP-activated protein kinase is a site 2 glycogen synthase kinase in skeletal muscle and is responsive to glucose loading. *Diabetes* **53**, 3074-3081.
Karlberg, O., Canback, B., Kurland, C. G. and Andersson, S. G. (2000). The dual origin of the yeast mitochondrial proteome. *Yeast* **17**, 170-187.
Kawata, T., Shevchenko, A., Fukuzawa, M., Jermyn, K. A., Totty, N. F., Zhukovskaya, N. V., Sterling, A. E., Mann, M. and Williams, J. G. (1997). SH2 signaling in a lower eukaryote: a STAT protein that regulates stalk cell differentiation in *Dictyostelium*. *Cell* **89**, 909-916.
Kikuno, R., Nagase, T., Nakayama, M., Koga, H., Okazaki, N., Nakajima, D. and Ohara, O. (2004). HUGE: a database for human KIAA proteins, a 2004 update integrating HUGEppi and ROUGE. *Nucleic Acids Res.* **32**, D502-D504.
Klein, G., Cotter, D. A., Martin, J. B. and Satre, M. (1990). A natural-abundance ^{13}C-NMR study of *Dictyostelium discoideum* metabolism – monitoring of the spore germination process. *Eur. J. Biochem.* **193**, 135-142.
Komatsu, M., Chiba, T., Tatsumi, K., Iemura, S., Tanida, I., Okazaki, N., Ueno, T., Kominami, E., Natsume, T. and Tanaka, K. (2004). A novel protein-conjugating system for Ufm1, a ubiquitin-fold modifier. *EMBO J.* **23**, 1977-1986.
Kotsifas, M., Barth, C., de Lozanne, A., Lay, S. T. and Fisher, P. R. (2005). Chaperonin 60 and mitochondrial disease in *Dictyostelium*. J. Muscle Res. Cell Motil. **23**, 839-852.
Liu, W., Shen, X., Yang, Y., Yin, X., Xie, J., Yan, J., Jiang, J., Wang, H., Sun, M., Zheng, Y. et al. (2004). Trihydrophobin 1 is a new negative regulator of A-Raf kinase. *J. Biol. Chem.* **279**, 10167-10175.
Mager, W. H. and Winderickx, J. (2005). Yeast as a model for medical and medicinal research. *Trends Pharmacol. Sci.* **26**, 265-273.
Matsuyama, S. I. and Maeda, Y. (1998). A mitochondrion as the structural basis of the formation of a cell-type-specific organelle in *Dictyostelium* development. *Protoplasma* **201**, 172-179.
Meton, I., Egea, M., Fernandez, F., Eraso, M. C. and Baanante, I. V. (2004). The N-terminal sequence directs import of mitochondrial alanine aminotransferase into mitochondria. *FEBS Lett.* **566**, 251-254.
Nakai, K. and Horton, P. (1999). PSORT: a program for detecting the sorting signals of proteins and predicting their subcellular localization. *Trends Biochem. Sci.* **24**, 34-35.
Nuckolls, G. H., Osherov, N., Loomis, W. F. and Spudich, J. A. (1996). The *Dictyostelium* dual-specificity kinase splA is essential for spore differentiation. *Development* **122**, 3295-3305.
Pang, K. M., Lynes, M. A. and Knecht, D. A. (1999). Variables controlling the expression level of exogenous genes in *Dictyostelium*. *Plasmid* **41**, 187-197.
Pendergrass, W., Wolf, N. and Poot, M. (2004). Efficacy of MitoTracker Green and CMXrosamine to measure changes in mitochondrial membrane potentials in living cells and tissues. *Cytometry* **61**, 162-169.
Raper, K. B. (1937). Growth and development of *Dictyostelium discoideum* with different bacterial associates. *J. Agric. Res.* **55**, 289-316.
Rutherford, C. L. and Harris, J. F. (1976). Localization of glycogen phosphorylase in specific cell types during differentiation of *Dictyostelium discoideum*. *Arch. Biochem. Biophys.* **175**, 453-462.
Schilde, C., Araki, T., Williams, H., Harwood, A. and Williams, J. G. (2004). GSK3 is a multifunctional regulator of *Dictyostelium* development. *Development* **131**, 4555-4565.
Schindler, J. and Sussman, M. (1977). Ammonia determines the choice of morphogenetic pathways in *Dictyostelium discoideum*. *J. Mol. Biol.* **116**, 161-169.
Shaulsky, G. and Loomis, W. F. (1993). Cell type regulation in response to expression of ricin-A in *Dictyostelium*. *Dev. Biol.* **160**, 85-98.
Spudich, J. A. (1987). *Methods in Cell Biology – Dictyostelium discoideum*: *Molecular Approaches to Cell Biology*. Orlando: Academic Press.
Sussman, M. (1987). Cultivation and synchronous morphogenesis of *Dictyostelium* under controlled experimental conditions. *Methods Cell Biol.* **28**, 9-29.
van Es, S., Wessels, D., Soll, D. R., Borleis, J. and Devreotes, P. N. (2001). Tortoise, a novel mitochondrial protein, is required for directional responses of Dictyostelium in chemotactic gradients. *J. Cell Biol.* **152**, 621-632.
Virdy, K. J., Sands, T. W., Kopko, S. H., Van Es, S., Meima, M., Schaap, P. and Cotter, D. A. (1999). High cAMP in spores of *Dictyostelium discoideum:* association with spore dormancy and inhibition of germination. *Microbiology* **145**, 1883-1890.
Wilczynska, Z., Barth, C. and Fisher, P. R. (1997). Mitochondrial mutations impair signal transduction in *Dictyostelium discoideum* slugs. *Biochem. Biophys. Res. Commun.* **234**, 39-43.
Williams, J. G., Noegel, A. A. and Eichinger, L. (2005). Manifestations of multicellularity: *Dictyostelium* reports in. *Trends Genet.* **21**, 392-398.
Wilson, J. B. and Rutherford, C. L. (1978). ATP, trehalose, glucose and ammonium ion localization in the two cell types of *Dictyostelium discoideum*. *J. Cell. Physiol.* **94**, 37-48.
Young, L. H., Li, J., Baron, S. J. and Russell, R. R. (2005). AMP-activated protein kinase: a key stress signaling pathway in the heart. *Trends Cardiovasc. Med.* **15**, 110-118.